Published in final edited form as:
Cytometry A. 2013 February ; 83(2): 227–234. doi:10.1002/cyto.a.22228.

Real-time cell viability assays using a new anthracycline derivative DRAQ7®

Jin Akagi[1], **Magdalena Kordon**[2], **Hong Zhao**[3], **Anna Matuszek**[1], **Jurek Dobrucki**[2], **Rachel Errington**[4], **Paul J Smith**[4], **Kazuo Takeda**[5], **Zbigniew Darzynkiewicz**[3], and **Donald Wlodkowic**[1,6,*]

[1]The BioMEMS Research Group, School of Chemical Sciences, University of Auckland, Auckland, New Zealand [2]Division of Cell Biophysics, Faculty of Biochemistry, Biophysics and Biotechnology, Jagiellonian University, Krakow, Poland [3]Brander Cancer Research Institute and Department of Pathology, New York Medical College, Valhalla, NY, USA [4]School of Medicine, Cardiff University, Cardiff, United Kingdom [5]On-chip biotechnologies Co. Ltd, Tokyo, Japan [6]School of Applied Sciences, RMIT University, Melbourne, Australia

Abstract

The exclusion of charged fluorescent dyes by intact cells has become a well-established assay for determining viability of cells. In search for a non-invasive fluorescent probe capable of long-term monitoring of cell death in real-time, we evaluated a new anthracycline derivative DRAQ7. The novel probe does not penetrate the plasma membrane of living cells but when the membrane integrity is compromised, it enters and binds readily to nuclear DNA to report cell death. It proved to be non-toxic to a panel of cancer cell lines grown continuously for up to 72 hours and did not induce any detectable DNA damage signaling when analyzed using laser scanning microscopy and flow cytometry. DRAQ7 provided a sensitive, real-time readout of cell death induced by a variety of stressors such as hypoxia, starvation and drug-induced cytotoxicity. The overall responses to anti-cancer agents and resulting pharmacological dose-response profiles were not affected by the growth of tumor cells in the presence DRAQ7. Moreover, we for the first time introduced a near real-time microflow cytometric assay based on combination of DRAQ7 and mitochondrial inner membrane potential ($\Delta\Psi_m$) sensitive probe TMRM. We provide evidence that this low-dosage, real-time labeling procedure provides multi-parameter and kinetic fingerprint of anti-cancer drug action.

Keywords

DRAQ7; real-time assays; cell viability; drug; cytotoxicity; DNA damage response; cell cycle; microfluidic; cytometry

INTRODUCTION

Tumor cell death serves as a useful end-point in the pharmacological profiling of cytotoxic and pro-apoptotic agents (1–4). Most contemporary cell viability assays are, however, performed using an “end-point” approach that reveals the frequency of live versus dead cells at the time of harvesting (5–7). Cell death within cell populations is, however, a stochastic process where cell-to-cell variation in temporal progression through the various stages of

*Corresponding author: The BioMEMS Research Group, School of Chemical Sciences, University of Auckland, Auckland, New Zealand; d.wlodkowic@auckland.ac.nz.

cell death arises from subtle fluctuations in the concentrations or the states of regulatory proteins, protein oscillations, the induction of multiple compensatory mechanisms (e.g. autophagy), or 'molecular noise' (7–11). Therefore, the ability to continuously track individual cells from the time of encountering a stress signal; through the execution phases of cell death, up to the final point of demise, can provide a kinetic fingerprint of anti-cancer drug action (3,6,7).

It was recently proposed that an ideal approach to monitor cell viability would require the development of non-invasive fluorescent markers that: (i) enable population monitoring and cell tracking over an extended period of time; (ii) do not by themselves modify the viability of the cell system, particularly the structural and bio-physiological properties of the cells; (iii) enable multi-parameter analysis in combination with other markers; and (iv) are transferable to high-throughput formats and automation (3,6–8,12).

In search for non-invasive fluorescent probes capable of long-term monitoring of cell death in real-time, we evaluated a new anthracycline derivative, DRAQ7. The probe does not penetrate plasma membrane of living cells, however once the membrane integrity is compromised, it readily binds to nuclear DNA and thus reports cell death. The spectral properties of the molecule provide a detection window in the far-red (>630nm) (identical to the cell permeant dye DRAQ5). The current study investigated the effects of DRAQ7 on living cells; its intracellular distribution and/or compartmentalization, the effects on cell cycle including DNA replication and possible interaction with genomic DNA that could be detected by the DNA damage response as measured by histone H2AX and ATM kinase phosphorylation. We found that real-time DRAQ7 assay reported the death of cells cultured under variety of perturbation and the overall responses to cytotoxic agents and resulting pharmacological dose-response profiles were not affected by the growth of cancer cells in the presence DRAQ7. Moreover, we for the first time introduced a near real-time microflow cytometric assay incorporating both the DRAQ7 and a mitochondrial membrane potential ($\Delta\Psi_m$) sensitive probe TMRM. In this regard we provide proof-of-concept evidence that such real-time labeling procedure can provide multi-parameter and kinetic fingerprints of anti-cancer drug action.

MATERIALS AND METHODS

Culture and treatments

A549 cells were purchased from American Type Culture Collection (ATCC #CCL-185, Manassas, VA). The cells were cultured in Ham's F12K medium with 2 mM L-glutamine adjusted to contain 1.5 g/L sodium bicarbonate (ATCC) supplemented with 10% fetal bovine serum (ATCC). Dual-chambered slides (Nunc Lab-Tek II) were seeded with 10^5 cells/ml suspended in 2 ml medium per chamber. The cells were maintained in exponential phase of growth, then treated with 3 μM DRAQ7 (Biostatus Ltd, Shepshed, UK) for a designated time followed by a wash step with phosphate buffered salt solution (PBS) and fixed by transferring slides into Coplin jars containing 1% methanol-free formaldehyde (Polysciences, Warrington, PA) for 15 min. The slides were rinsed with PBS and kept at −20° C in 70% ethanol until required for further staining.

U937 and THP1α cell lines were cultured in a complete Advanced RPMI 1640 culture medium supplemented with 5% FBS as described previously (5,13,14). For quantification of drug-induced cytotoxicity 2.5×10^5 cells/ml of cells were suspended in 1 ml of medium and treated with cell cycle inhibitors and apoptosis inducers Staurosporine (STS; Life Technologies; 0.01–1 μM), Etoposide (ETO; Merck Millipore; 100–1000 μM), Actinomycin D (Act D; Merck Millipore, Billerica, MA, USA; 0.001–1 μM), Cycloheximide (CHX; Merck Millipore; 100–1000 μM) and small-molecule BH3 mimetics

ABT-737 (Selleckchem, Houston, TX, USA; 0–7.5 μM) and TW37 (Selleckchem; 0–25 μM). This was followed by staining with cell impermeable DNA-stains at the end of experiment (end-point assay; 5 min at RT with 1 μg/ml of PI, 100 nM of SYTOX Red or 3 μM of DRAQ7). Alternatively, cells were cultured in the presence of 3 μM of DRAQ7 and regularly examined during the course of the experiment (dynamic assay) by flow cytometry as described below.

Confocal microscopy

HeLa cells expressing the eGFP-tagged linker histone H1 (15) were cultured on round coverslips (thickness 0.17 mm, 22 mm in diameter, Menzel-Gläser, Braunschweig, Germany) submerged in Petri dishes (40 mm in diameter). The treated cells were cultured and imaged in Dulbecco's MEM (Sigma) supplemented with 10% fetal bovine serum (Sigma), Phenol Red and antibiotics (penicillin and streptomycin). DMEM was buffered for 5% CO_2 in the atmosphere. The concentration of DRAQ7 was 3 μM unless otherwise stated. In cells cultured under suboptimal conditions, DMEM was substituted by DMEM/F-12 with 2% FBS. Concentration of DRAQ7 in these experiments was 3, 5 or 10 μM. Coverslips with cells were mounted in a custom-made steel holder and the sample was placed on a microscope stage and imaged using a Leica TCS SP5 confocal laser-scanning microscope, equipped with stage microincubator.

Detection of H2AX and ATM Phosphorylation

Slides (from above) were washed twice in PBS and the cells on the slides treated with 0.1% Triton X-100 (Sigma) in PBS for 15 min, and with a 1% (w/v) solution of bovine serum albumin (BSA; Sigma) in PBS for 30 min to suppress nonspecific antibody (Ab) binding. The cells were then incubated in a 100 μl volume of 1% BSA containing a 1:300 dilution of phospho-specific (Ser139) γH2AX mAb (BioLegend, San Diego, CA) or 1:200 dilution of phosphor-specific (Ser1981) ATM mAb (Merck Millipore) overnight at 4°C. The secondary AlexaFluor 488 fluorochrome (Life Technologies, at a dilution of 1:100) and incubated for 45min at room temperature. Before measurement by laser scanning cytometry (LSC), the cells were counterstained with 2.8 μg/ml 4,6-diamidino-2-phenylindole (DAPI; Sigma) in PBS for 15 min. Each experiment was performed with an IgG control in which cells were labeled with the secondary AlexaFluor 488 Ab only; without primary antibody incubation to estimate the extent of nonspecific binding of the secondary antibody to the cells. Other details of cell labeling with the primary and secondary Ab have been previously described (16,17).

Flow Cytometry

Flow cytometry was performed using a Fishman-R microfluidic flow cytometer (On-chip biotechnologies Co. Ltd, Tokyo, Japan) equipped with 473 and 640 nm solid-state lasers and integrated digital data processing (18–20). Logarithmic amplification scale using following configuration of band-pass (BP) filters was applied: (i) 473 nm excitation line: FL2 channel (585 BP for collection of PI and TMRM signals); (ii) 640 nm excitation line: FL4 channel (690 BP for collection of: DRAQ7 fluorescence signals). A typical run used a sample with 5000–10000 cells. Native data files were converted to FCS 3.0 standard using Fishman-R data converter.

Data and Statistical Analysis

Data analysis and presentation was performed using FCS Express 4 RUO Flow Cytometry (De Novo Software) software. Pharmacological dose response curves and IC50 values were plotted using GraphPad Prism 5.0 (GraphPad Software Inc, La Jolla, USA) software.

Student's t and ANOVA tests were applied for comparison between groups with significance set at $p<0.01–0.05$.

RESULTS & DISCUSSION

DRAQ7 does not cause detectable cytotoxicity (acute or long-term)

Initial screening of U937 and THP1α cell lines with a dose range of 0.35 – 10 μM DRAQ7 was undertaken to assess the impact of the probe upon cell viability. When analyzed using microflow cytometer, all cells continuously grown in the presence of a DRAQ7, did not show any increase in basal fluorescence after 24 hours of exposure (Figure 1A, upper panel). This feature suggested that DRAQ7 as a viability probe could be particularly suitable for kinetic assays. It was also in contrast to our previously reported data on the spectrally dissimilar plasma membrane permeability marker propidium iodide (PI; 1 μg/ml; excitation at 488 nm, emission at 585 nm) where continuous culture of cells with PI led to a profound increase in overall cell fluorescence despite having no impact on cell viability (6). Most notably, the fluorescence levels of cells cultured with DRAQ7 were comparable to end-point staining with 1 μg/ml of PI (Figure 1A, bottom panel). Both U937 and THP1α cells remained viable when grown with the DRAQ7 probe as evidenced by the lack of cell subpopulations exhibiting enhanced fluorescence signal intensity in the top right quadrants (Figure 1A). Importantly even a 20 μM concentration of DRAQ7 proved to be non-toxic to both cell lines for up to 72 hours, also confirmed by the counterstaining with PI (Figures 1B–C). Moreover, no dysfunctions in the mitochondrial function were observed as assessed by the multiparameter labeling with $\Delta\Psi_m$ sensitive probe tertamethylrhodamine methyl ester (TMRM; 200 nM) at 24, 48 and 72 hours of incubation (Figure 1D). Most cells featured intact and energized mitochondria indicated by $TMRM^{high}$ and $DRAQ7^{neg}$ (deemed live) subpopulation in the upper left quadrant shown in the Figure 1D. Cell proliferation and cell cycle distribution were also not affected for up to 72 hours growth of cells in the presence of 3–5 μM DRAQ7 (data not shown).

In search of early signs of the dye entry, we also cultured HeLa cells expressing the eGFP-tagged linker histone H1 in the continuous presence of DRAQ7 (3 μM) for up to 72 hours. Cells were imaged using confocal microscopy to assess the dye penetration and signs of histone H1 dissociation. Even after 72 hours of continuous incubation DRAQ7 was not detected in cell nuclei (Figure 2A, Supplementary Figure 1). The absence of free intracellular DRAQ7 capable of reaching chromatin was also confirmed by the absence of detectable dissociation of eGFP-tagged histone H1 from DNA and subsequent chromatin aggregation. Next to demonstrate the suitability of DRAQ7 for real-time microscopic tracking and detection of cell death we imaged HeLa cells grown under starvation conditions in culture medium supplemented with reduced serum concentration and 3 μM of DRAQ7 (Figure 2B). Serum deprivation led to cell death detected by DRAQ7 incorporation within approximately 72 hours. DRAQ7 provided thus a straightforward and real-time marker to track the demise of individual cells under stress conditions using time-lapse confocal microscopy.

DRAQ7 does not induce DNA damage signaling

Next we set to explore a possible DNA damage signaling in response to DRAQ7. For this purpose A549 cells were maintained in cultures either untreated or treated with 3 μM of DRAQ7 for 4, 24 or 48 h. The induction of DNA damage signaling was measured as an increase in phosphorylation of H2AX on Ser139 (expression of γH2AX) and activation of ATM through its phosphorylation on Ser1981 (ATM-$S1981^P$) (Figure 3A and B). These phosphorylation events were detected with the use of respective phospho-specific antibodies, and cellular immunofluorescence measured by laser scanning cytometry (LSC).

The exposure of cells to DRAQ7 caused no detectable induction of γH2AX regardless of duration of the treatment (Figure 3). In fact, a minor decrease in expression of γH2AX was noted in the DRAQ7-treated cells. Also, no detectable effect of DRAQ7 was seen on the cell cycle distribution as revealed by the DNA content frequency histograms (Figure 3A, insets).

The effect of DRAQ7 on activation of ATM was assessed in an independent set of cultures (Figure 3B). Similar as in the case of γH2AX a decline of expression ATM-S1981^{P} after 4 and 24 h was seen in cells treated with DRAQ7. However, a minor increase of ATM activation was noted in cells incubated with DRAQ7 for 48 h. The extent of this increase is much lower than in the case of other supravital probes such as PI, DRAQ5 or Hoechst 33342 (21). In this set of cultures also no evidence of a change in cell cycle distribution in cells exposed to DRAQ7 that would be reflected by the DNA content frequency histograms (Figure 3B, insets) was apparent.

DRAQ7 can be applied in real-time viability assays

Based on the above results, we next determined the applicability of DRAQ7 probe for the quantification of pharmacologically induced cell death based on real-time assay principle and cell sampling using innovative microfluidic flow cytometer (18,22,23). Potential interactions between fluorescent probes and cytotoxic drugs can introduce possible bias in estimating the toxic effects in dynamic real-time assays (6,12,22). To exclude this possibility, we therefore investigated a panel of cytotoxic drugs and apoptotic inducers on human hematopoietic tumor cell lines. Initially THP1α cells were exposed to a panel of apoptosis inducers: staurosporine (STS), etoposide (ETO), actinomycin D (AD) and small-molecule Bcl-2 inhibitors ABT-737 and TW37 for up to 24h, at the drug concentrations described in the Methods (Figure 4A–B). The cells were grown in the continuous presence of 3 μM DRAQ7 and the indicated inducers of apoptosis (Figure 4A–B). Following 24-hour of growth cells were aspirated and immediately sampled in complete medium by the microfluidic flow cytometry at the end of the experiment without any additional washing steps. The results were compared with conventional end-point assays where cell samples were probed using DRAQ7 (3 μM), PI (1 μg/ml) and SYTOX Red (SXR; 100 nM) staining at the end of the experiment (Figure 4A–B). Our results indicated that responses of tumor cells to various cytotoxic and pro-apoptotic stimuli were not affected by the growth in the continuous presence of DRAQ7 probe. The calculated IC50 values for STS were 0.05, 0.04, 0.05 and 0.05 for the real-time DRAQ7, end-point DRAQ7, PI and SXR assays, respectively. The calculated IC50 values for ETO were 4.3, 4.5, 4.2 and 3.9 for the real-time DRAQ7, end-point DRAQ7, PI and SXR assays, respectively (Figure 4A–B). In both instances the differences between IC50 values obtain with real-time and end-point protocols were considered not statistically significant (ANOVA; $p<0.01$) and corresponded to Pearson linear correlation R^2 values greater than 0.98.

These promising results prompted us to expand our bioassay development approach to incorporate a two-color real-time assay utilizing both the DRAQ7 and a $\Delta\Psi_m$ sensitive probe TMRM (Figure 4C) (1,24). The latter probe is inert to many human cell lines at concentrations not exceeding 500 nM when grown in continuous presence of the probe for up to 72h. This offers a unique capability to perform real-time monitoring of mitochondrial membrane inner membrane potential without any additional staining and washing steps. Accordingly, we have combined both probes to provide a multi-parameter readout of caspase-dependent apoptosis induced by small-molecule drugs. Upon treatment with the apoptosis inducer AD, the real-time DRAQ7 / TMRM assay provided similar estimates of the three cell populations: TMRM^{high} / DRAQ7^{neg} (deemed live), TMRM^{low} / DRAQ7^{neg} (deemed early apoptotic), and TMRM^{low} / DRAQ7^{high} (deemed late apoptotic/necrotic) as the data obtained using conventional end-point protocols (Figure 4C; Pearson linear correlation $R^2 = 0.98 – 0.99$). The calculated IC50 values based on cell viability estimates

for the small molecule Bcl-2 inhibitor ABT-737 were 2.26 and 2.10 using the DRAQ7 / TMRM real-time vs. end-point assays, respectively (Figure 4D). The calculated IC50 values based on cell viability estimates for the small molecule Bcl-2 inhibitor TW37 were 1.79 and 1.46 using the DRAQ7 / TMRM real-time vs. end-point assays, respectively (Figure 4E). In both instances the differences between IC50 values obtained with real-time vs. end-point protocols were considered not statistically significant (ANOVA; $p<0.01$ for ABT737 and $p<0.05$ for TW37) and corresponded to Pearson linear correlation R^2 values greater than 0.98 (Figure 4D–E).

The application of inert DRAQ7 and TMRM probes provided us also with an opportunity to investigate the kinetic properties of small-molecule Bcl-2 inhibitors such as TW37. Figure 4F depicts an on-demand, near-real-time microflow cytometric assay where cells were continuously grown in the presence of both probes on a chip-based device and then sampled (10–20 μl volume) every 5 minutes to provide the kinetic profile of drug action. Most notably we were able to demonstrate that even though the dissipation of $\Delta\Psi_m$ occurs within 10–15 min following challenge with BH3 mimetic TW37, the gradual loss of plasma integrity occurs only after 8 hours of stimulation while nearly 74% of cells can still be considered $TMRM^{low}/DRAQ7^{neg}$ after 24 hours (Figure 4F). This indicates that THP1 cells were able to compensate for the $\Delta\Psi_m$ loss for a considerable amount of time before committing to complete cell demise. These results reinforce our earlier studies on small-molecule BH3 mimetic HA14-1 in follicular lymphoma cells indicating a relatively transient character of $\Delta\psi_m$ loss and potential involvement of compensatory mechanisms (1,2,25). The latter can be based on the multiple switches between slow but also variable in time decision-making processes, involving gradual accumulation of pro-apoptotic molecules (e.g., tBid, Bax complexes), followed by snap-action rapid activation of caspases, and variable kinetics and specificity of proteolytic degradation of endogenous targets as reported recently (7–9).

CONCLUSIONS

In search for the non-invasive fluorescent probes capable of long-term monitoring of cell death in real-time, we developed and evaluated a new anthracycline derivative, DRAQ7. DRAQ7 being a far-red fluorescent DNA dye exhibits convenient spectral properties that allow for multiplexing with makers such as GFP, FITC and Cy3. Once the membrane integrity is compromised, DRAQ7 binds readily to nuclear DNA with high affinity and reports cell death by strong far-red fluorescence. Our data indicated that the growth, cell cycle distribution and proliferation of several tumor cell lines were unaffected by the continuous presence of DRAQ7 for up to 3 days of culture. Also, unlike other DNA supravital probes (21), continuous incubation with DRAQ7 led to no evidence of either DNA damage, replication stress or induction of cell senescence (26).

Collectively, data lend a strong support to real-time pharmacological profiling using DRAQ7 (6,12). In such assays, the fluorescence markers, applied supravitally, should have a minimal effect on structure, function and survival of the cells being studied. Lack of any noticeable influence on cell responses to or interaction with cytotoxic agents during growth in the presence of DRAQ7 allows for a direct adaptation for the automated and real-time pharmacological profiling of anti-cancer drugs. Importantly, a substantial reduction of sample processing steps and avoidance of washing protocols achieved with such a kinetic protocol is important for the preservation and retrieval of fragile cell subpopulations. We conclude that the current data provide a foundation for the development of a new generation of cell viability assays with vast applications in both flow and imaging cytometry.

Supplementary Material

Refer to Web version on PubMed Central for supplementary material.

Acknowledgments

Grant sponsor: Supported by the Faculty Research Development Fund, University of Auckland (JA, DW); Early Career Research Excellence Award, University of Auckland (DW); Ministry of Science and Innovation (MSI), New Zealand (JA, DW); On-chip biotechnologies Co Ltd (JA, AM, KT, DW); NCN grant UMO-2011/01/B/NZ3/00609), EU structural funds grant BMZ no. POIG.02.01.00-12-064/08. (MK, JD); NCI CA RO1 28 704 (HZ, ZD); EPSRC Basic technology grant No EP/F040954/1 (RE, PJS).

References

1. Wlodkowic D, Skommer J, Pelkonen J. Multiparametric analysis of HA14-1-induced apoptosis in follicular lymphoma cells. Leuk Res. 2006; 30:1187–92. [PubMed: 16414117]
2. Wlodkowic D, Skommer J, Pelkonen J. Brefeldin A triggers apoptosis associated with mitochondrial breach and enhances HA14-1- and anti-Fas-mediated cell killing in follicular lymphoma cells. Leuk Res. 2007; 31:1687–700. [PubMed: 17428536]
3. Wlodkowic D, Skommer J, Darzynkiewicz Z. Cytometry in cell necrobiology revisited. Recent advances and new vistas. Cytometry A. 2010; 77:591–606. [PubMed: 20235235]
4. Darzynkiewicz Z, Juan G, Li X, Gorczyca W, Murakami T, Traganos F. Cytometry in cell necrobiology: analysis of apoptosis and accidental cell death (necrosis). Cytometry. 1997; 27:1–20. [PubMed: 9000580]
5. Khoshmanesh K, Akagi J, Nahavandi S, Skommer J, Baratchi S, Cooper JM, Kalantar-Zadeh K, Williams DE, Wlodkowic D. Dynamic analysis of drug-induced cytotoxicity using chip-based dielectrophoretic cell immobilization technology. Anal Chem. 2011; 83:2133–44. [PubMed: 21344868]
6. Zhao H, Oczos J, Janowski P, Trembecka D, Dobrucki J, Darzynkiewicz Z, Wlodkowic D. Rationale for the real-time and dynamic cell death assays using propidium iodide. Cytometry A. 2010; 77:399–405. [PubMed: 20131407]
7. Skommer J, Darzynkiewicz Z, Wlodkowic D. Cell death goes LIVE: technological advances in real-time tracking of cell death. Cell Cycle. 2010; 9:2330–41. [PubMed: 20519963]
8. Skommer J, Raychaudhuri S, Wlodkowic D. Timing is everything: stochastic origins of cell-to-cell variability in cancer cell death. Front Biosci. 2011; 16:307–14. [PubMed: 21196172]
9. Skommer J, Brittain T, Raychaudhuri S. Bcl-2 inhibits apoptosis by increasing the time-to-death and intrinsic cell-to-cell variations in the mitochondrial pathway of cell death. Apoptosis. 2010; 15:1223–33. [PubMed: 20563668]
10. Hawkins ED, Markham JF, McGuinness LP, Hodgkin PD. A single-cell pedigree analysis of alternative stochastic lymphocyte fates. Proc Natl Acad Sci U S A. 2009; 106:13457–62. [PubMed: 19633185]
11. Raychaudhuri S, Willgohs E, Nguyen TN, Khan EM, Goldkorn T. Monte Carlo simulation of cell death signaling predicts large cell-to-cell stochastic fluctuations through the type 2 pathway of apoptosis. Biophys J. 2008; 95:3559–62. [PubMed: 18641073]
12. Wlodkowic D, Faley S, Darzynkiewicz Z, Cooper JM. Real-time cytotoxicity assays. Methods Mol Biol. 2011; 731:285–91. [PubMed: 21516415]
13. Khoshmanesh K, Akagi J, Nahavandi S, Kalantar-zadeh K, Baratchi S, Williams DE, Cooper JM, Wlodkowic D. Interfacing cell-based assays in environmental scanning electron microscopy using dielectrophoresis. Anal Chem. 2011; 83:3217–21. [PubMed: 21443166]
14. Wlodkowic D, Faley S, Skommer J, McGuinness D, Cooper JM. Biological implications of polymeric microdevices for live cell assays. Anal Chem. 2009; 81:9828–33. [PubMed: 19902928]
15. Kanda T, Sullivan KF, Wahl GM. Histone-GFP fusion protein enables sensitive analysis of chromosome dynamics in living mammalian cells. Current biology : CB. 1998; 8:377–85. [PubMed: 9545195]

16. Zhao H, Rybak P, Dobrucki J, Traganos F, Darzynkiewicz Z. Relationship of DNA damage signaling to DNA replication following treatment with DNA topoisomerase inhibitors camptothecin/topotecan, mitoxantrone, or etoposide. Cytometry Part A. 2012; 81:45–51.

17. Zhao H, Dobrucki J, Rybak P, Traganos F, Dorota Halicka H, Darzynkiewicz Z. Induction of DNA damage signaling by oxidative stress in relation to DNA replication as detected using “click chemistry”. Cytometry Part A. 2011; 79:897–902.

18. Takao M, Takeda K. Enumeration, characterization, and collection of intact circulating tumor cells by cross contamination-free flow cytometry. Cytometry A. 2011; 79:107–17. [PubMed: 21246706]

19. Wlodkowic D, Khoshmanesh K, Sharpe JC, Darzynkiewicz Z, Cooper JM. Apoptosis goes on a chip: advances in the microfluidic analysis of programmed cell death. Anal Chem. 2011; 83:6439–46. [PubMed: 21630641]

20. Wlodkowic D, Cooper JM. Tumors on chips: oncology meets microfluidics. Curr Opin Chem Biol. 2010; 14:556–67. [PubMed: 20832352]

21. Zhao H, Traganos F, Dobrucki J, Wlodkowic D, Darzynkiewicz Z. Induction of DNA damage response by the supravital probes of nucleic acids. Cytometry A. 2009; 75:510–9. [PubMed: 19373929]

22. Wlodkowic D, Skommer J, McGuinness D, Faley S, Kolch W, Darzynkiewicz Z, Cooper JM. Chip-based dynamic real-time quantification of drug-induced cytotoxicity in human tumor cells. Anal Chem. 2009; 81:6952–9. [PubMed: 19572560]

23. Wlodkowic D, Skommer J, Faley S, Darzynkiewicz Z, Cooper JM. Dynamic analysis of apoptosis using cyanine SYTO probes: from classical to microfluidic cytometry. Exp Cell Res. 2009; 315:1706–14. [PubMed: 19298813]

24. Floryk D, Houstek J. Tetramethyl rhodamine methyl ester (TMRM) is suitable for cytofluorometric measurements of mitochondrial membrane potential in cells treated with digitonin. Bioscience reports. 1999; 19:27–34. [PubMed: 10379904]

25. Skommer J, Wlodkowic D, Matto M, Eray M, Pelkonen J. HA14-1, a small molecule Bcl-2 antagonist, induces apoptosis and modulates action of selected anticancer drugs in follicular lymphoma B cells. Leuk Res. 2006; 30:322–31. [PubMed: 16213584]

26. Zhao H, Halicka HD, Traganos F, Jorgensen E, Darzynkiewicz Z. New biomarkers probing depth of cell senescence assessed by laser scanning cytometry. Cytometry Part A. 2010; 77:999–1007.

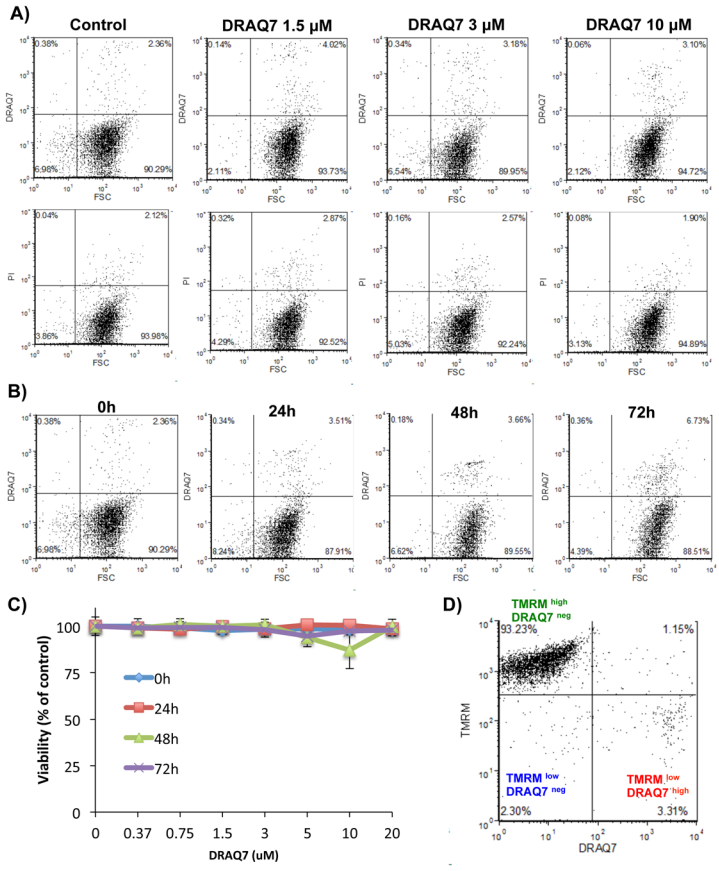

Figure 1.

DRAQ7 probe is non-toxic over a wide concentration range**. A)** THP1α cells were treated with 0.35 – 10 μM of DRAQ7 for up to 24 hours to assess impact of the dye upon cell viability. The fluorescence levels of cells cultured with DRAQ7 were comparable to end-point staining with 1 μg/ml of PI (bottom panel). Both U937 and THP1α cells remained viable when grown with DRAQ7 probe as evidenced by the lack of cell subpopulation exhibiting enhanced fluorescence signal intensity in the top right quadrants. **B)** The extreme concentration of DRAQ7 (20 μM) is non-toxic to THP1α cells for up to 72 hours of continuous exposure. **C)** Comparative analysis of cell viability across the broad range of doses and incubation times. Data were derived from a $DRAQ7^{neg}$ gate (deemed live) and cross-validated with counterstaining with a spectrally dissimilar plasma membrane permeability stain PI (1 μg/ml). **D)** Mitochondrial function is not affected in THP1α cells cultured for up to 72 hours with 20 μM of DRAQ7 as assessed by the multiparameter labeling with $\Delta\Psi_m$ sensitive probe tertamethylrhodamine methyl ester (TMRM; 200 nM). Most cells featured intact and energized mitochondria indicated by $TMRM^{high}$ and $DRAQ7^{neg}$ (deemed live) subpopulation in the upper left quadrant.

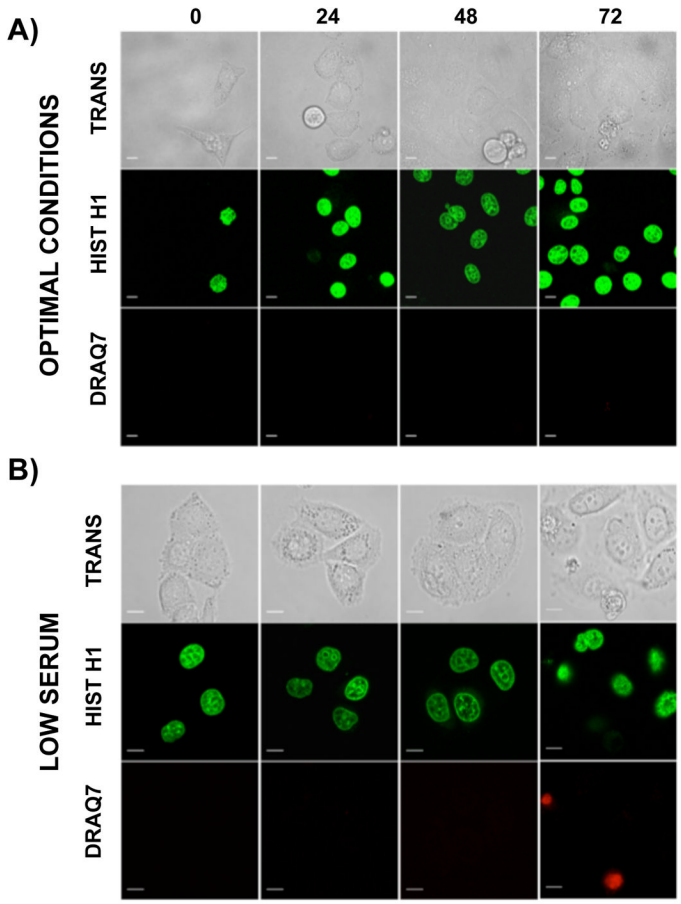

Figure 2.

Confocal microscopy studies of DRAQ7 reporting cell death. Transmitted light images, fluorescence images of GFP-tagged histone H1, and images of DRAQ7 in cells grown under optimal conditions (**A**), in medium with a low concentration (2%) of serum (**B**). A loss of plasma membrane integrity is reported by DRAQ7 entering and staining the nuclear DNA. Images were collected using the scan speed of 100 Hz, except for the frames presented in panel A (0h, 24h, 48h) where the scan speed was 400Hz. The brightness, contrast and γ function were adjusted in fluorescence images of DRAQ7 $\gamma = 0.5$; in images of GFP-tagged histone H1 $\gamma = 0.75$. Processing was required to visualize the weak fluorescence signals of DRAQ7. Scale bars: 10 μm.

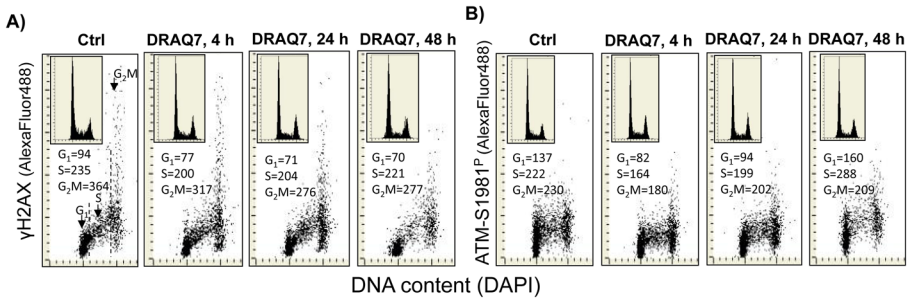

Figure 3.

Effects of prolonged cell culture with DRAQ7 on DNA damage responses. **A)** Expression of γH2AX of A549 cells, untreated (Ctrl) and exposed to 3 μM DRAQ in cultures for 4, 24 and 48 h. The mean values of γH2AX expression estimated for subpopulations of cells in G_1, S and G_2M phases of the cell cycle are shown in the respective panels. The insets present DNA content frequency histograms from the respective cultures. **B)** Expression of ATM-S1981^P of A549 cells, untreated (Ctrl) and exposed to 3 μM DRAQ7 in cultures for 4, 24 and 48 h. The mean values of ATM-S1981^P expression estimated for subpopulations of cells in G_1, S and G_2M phases of the cell cycle are shown in the respective panels. The insets present DNA content frequency histograms from the respective cultures.

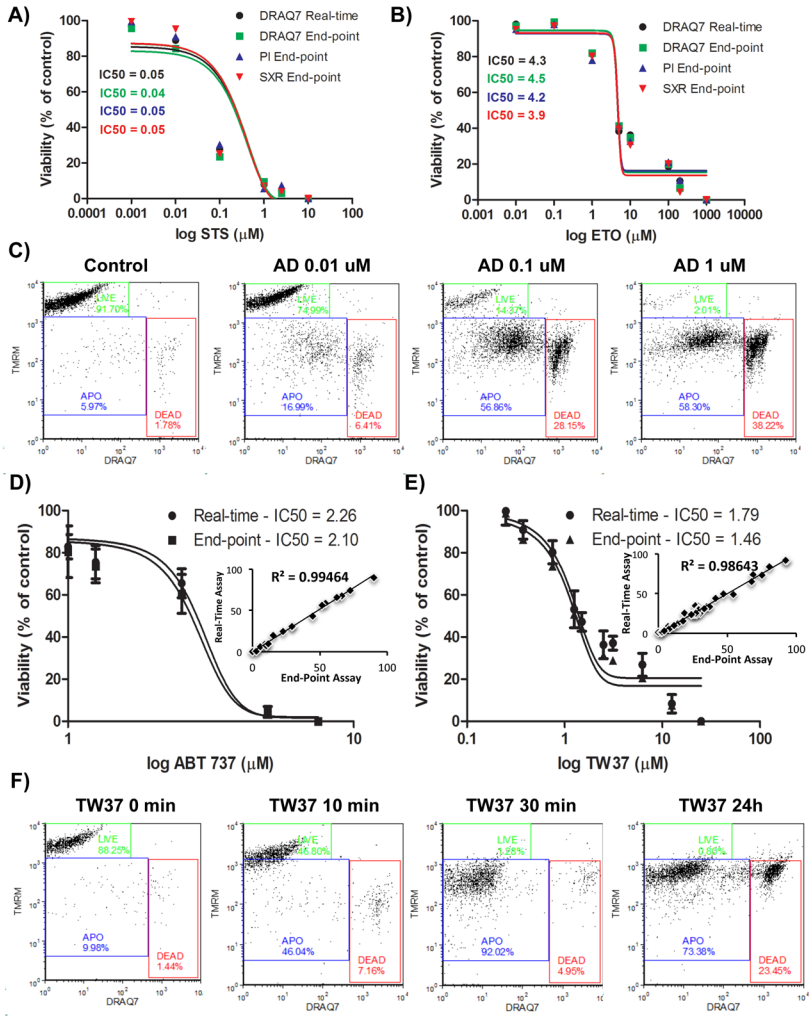

Figure 4.

Pharmacological profiling is not affected by the growth of hematopoietic cancer cells in the continuous presence of DRAQ7 probe. **A)** THP1α were challenged for up to 24 hours with increasing doses of staurosporine (STS) in the presence of 3 μM DRAQ7 (real-time assay). For comparison cell were also analyzed using standard (end-point) assay using 3 μM of DRAQ7, 1 μg/ml of PI and 100 nM of SYTOX Red probe as described under Materials and Methods. Curve fitting and IC50 values were calculated by plotting the data from $DRAQ7^{neg}$ gate (deemed live). **B)** THP1α were challenged for up to 24 hours with increasing doses of Etoposide (ETO) in the presence of 3 μM DRAQ7 (real-time assay). For comparison cell were also analyzed using standard (end-point) assays as described in A. Data analysis was performed analogically to conditions shown on A. **C)** THP1α were challenged for up to 24 hours with increasing doses of Actinomycin D (AD) in the presence of 3 μM DRAQ7 and 200 nM of ($\Delta\Psi_m$ sensitive probe TMRM real-time assay) and immediately sampled in complete medium using the microfluidic chip-based cytometer. **D)** THP1α cells were challenged for up to 24 hours with increasing doses of small-molecule Bcl-2 inhibitor ABT-737 in the presence of 3 μM DRAQ7 and 200 nM of $\Delta\Psi_m$ sensitive probe TMRM (real-time assay). Alternatively cells were labeled using an end-point static assay with identical DRAQ7 concentrations. Pharmacological dose-response curve fitting and IC50 calculations were performed using data from $TMRM^{high}$ / $DRAQ7^{neg}$ gate (deemed live; LIVE). Inset shows a cumulative Pearson linear correlation analysis of all data

acquired from gates $TMRM^{high}$ / $DRAQ7^{neg}$ (deemed live; LIVE), $TMRM^{low}$ / $DRAQ7^{neg}$ (deemed apoptotic; APO), and $TMRM^{low}$ / $DRAQ7^{high}$ (deemed late apoptotic/necrotic; DEAD). **E)** THP1α cells were challenged for up to 24 hours with increasing doses of small-molecule Bcl-2 inhibitor TW-37. Condition and data analysis were identical to these described in D. For A–E note excellent agreement between results obtained with end-point vs. real-time no-wash protocols that indicates no interactions between the probe and anti-cancer drugs (Pearson linear correlation $R^2 = 0.98–99$ at $p<0.01$). **F)** Kinetic analysis of small-molecule Bcl-2 inhibitor TW37 using real-time DRAQ7 (3 μM) / TMRM (200 nM) assay and time-lapse sampling using microfluidic chip-based cytometer. Note that even though the dissipation of $\Delta\Psi_m$ occurs within 10–15 min following challenge with BH3 mimetic TW37, the gradual loss of plasma integrity occurs only after 8 hours of stimulation while nearly 74% of cells can sill be considered $TMRM^{low}$/$DRAQ7^{neg}$ after 24 hours.